Sensitivity of second harmonic generation to space charge effects at Si(111)/electrolyte and Si(111)/SiO_2/electrolyte interfaces

P. R. Fischer, J. L. Daschbach, D. E. Gragson, and G. L. Richmond
Department of Chemistry, University of Oregon, Eugene, Oregon 97403

(Received 11 October 1993; accepted 15 June 1994)

The potential dependence in the surface second harmonic response from hydrogen terminated n-Si(111) and oxidized n-Si(111) surfaces has been examined in aqueous NH_4F and H_2SO_4 solutions. The relative phase of the nonlinear response as measured by rotational anisotropy experiments is found to be highly sensitive to the presence of the oxide and the field applied across the Si(111)/oxide/electrolyte interface. These observations are attributed to field effects within the space–charge region of the semiconductor which vary with the presence and thickness of the insulating oxide layer on the Si(111) surface.

I. INTRODUCTION

Understanding the electrochemical behavior of semiconductor surfaces remains challenging due to the highly reactive nature of these surfaces. Nevertheless, studies continue to be performed in this area because of the technological importance of these materials, particularly Si and GaAs. In recent years, significant progress has been made in characterizing the silicon surface and the silicon/electrolyte interface by infrared reflectance,[1,2] ultrahigh vacuum (UHV) transfer experiments,[3,4] scanning tunneling microscope (STM),[5–10] and atomic force microscope (AFM)[11] imaging. Many of these studies have taken advantage of the relative stability to oxidation of silicon surfaces prepared in a hydrogen terminated state. Much less is known about the oxidized Si surface frequently found in both air and water owing to the inapplicability of many of the above techniques for examining the buried Si/SiO_2 interfacial region. The presence of this oxide can significantly alter the electrochemistry and the electronic properties of the semiconductor, as it both insulates the surface and is capable of storing significant charge. Second harmonic generation (SHG) provides an alternative means of examining the silicon surface and buried Si/SiO_2 interface.[12–14]

In this article, we discuss the application of optical SHG to studying Si(111)/electrolyte and Si(111)/SiO_2/electrolyte interfaces for which oxides have been photoanodically grown on the surface. There are two primary objectives in this study. The first is to correlate the intensity and relative phase of the SH optical response with the potential induced variations in the static field applied to the semiconductor/electrolyte interface, and related to this, how the presence of oxide layers of varied thicknesses on the Si(111) surface alters this potential dependence. Unlike metal electrodes, where SHG is highly sensitive to potential variation due to the screening of the charge at the surface,[15,16] the field for semiconductors can extend several hundred angstroms into the material, the depth being dependent upon the doping density of the semiconductor, possible Fermi-level pinning, and the strength of the applied field.

The second focus of this study has been of a more fundamental nature. That is to address issues related to the source of the response from these buried interfaces, the relative contributions from the depletion layer, the Si(111) surface adjacent to the electrolyte or oxide, and the SiO_2 layer, as well as determining the coupling of the applied static field to various susceptibility tensors. For semiconductors, the bulk response can be significant and thus any study which attempts to understand the source of the response must be concerned with the higher order terms. In the present study, this issue has been addressed by potential dependent measurements.

The H–Si(111) and the oxidized surface were examined in different electrolyte solutions and in UHV. Much of the work reported involves measuring the variation in the SH response with azimuthal rotation of the sample by 360° about its normal. The simplest system is a H-terminated sample examined under potential control in NH_4F. This surface should be monohydrogen terminated, smooth, and relatively free of any photogenerated surface oxides due to the solubility of the oxides in this solution.[17] The results obtained at the flatband potential are compared with similar rotational anisotropy measurements conducted in UHV for a sputtered and annealed sample, and a hydrogen terminated sample transferred to UHV without further surface cleaning. These studies are followed by potential dependent measurements of the SH rotational anisotropy from initially H-terminated surface immersed in a H_2SO_4 solution where, unlike the NH_4F solution, the surface oxides which are formed photoanodically are insoluble. Similarly, experiments are conducted on samples immersed in H_2SO_4 on which controlled amounts of surface oxides (0–40 Å) are photoanodically grown prior to examination of the SH potential dependence.

II. DESCRIPTION OF SHG FROM CUBIC MEDIA

When the electromagnetic field polarizes a medium, this interaction is governed by Maxwell's equations and the constitutive relations. The second order polarization that gives rise to SHG can be expressed by a series of multipole terms,[18,19]

 0734-2101/94/12(5)/2617/8/$1.00 ©1994 American Vacuum Society

$$\mathbf{P}_{\text{eff}}^{(2)}(2\omega)=\chi^{D}:E(\omega)E(\omega)+\chi^{P}:E(\omega)\nabla E(\omega)$$
$$-\nabla\chi^{Q}:E(\omega)E(\omega)-\chi^{Q}:\nabla E(\omega)E(\omega)$$
$$+\frac{c}{i2\omega}\nabla[\chi^{M}:E(\omega)E(\omega)], \qquad (1)$$

where χ represents the susceptibility tensor for each term and $E(\omega)$ represents the incident field. The first two terms are electric dipole in nature, the third and fourth describe the electric quadrupole contribution and the last term the magnetic dipole contribution. Under the electric dipole approximation, the second order response vanishes in the bulk of centrosymmetric media and is allowed only at the interface where the inversion symmetry is broken. When describing the in-plane response, only the first term should be considered since the tangential components of the incident electric field are continuous across the interface. However, if either the driving fields or the SH polarization under consideration contains a field component normal to the surface, then there will be contributions from the higher order terms to the surface response.

SHG derives its surface sensitivity from not only the dipole allowed surface terms, but higher order (quadrupole) terms which are inseparable from the dipole terms. The induced nonlinear surface polarization can be written in terms of an effective susceptibility as[20,21]

$$P_{\text{eff}}^{(2)}(2\omega)=\chi_{\text{eff}}^{(2)}:E(\omega)E(\omega), \qquad (2)$$

where $\chi_{\text{eff}}^{(2)}$ is the second order susceptibility tensor reflecting the optical as well as the symmetry properties of the surface layer and is comprised of contributions from the bulk and the surface. If the SH intensity is recorded as a function of azimuthal angle of rotation, the variation in intensity reflects the overall symmetry of the surface and allows determination of the tensorial properties of χ_{eff}.

The (111) surface, which is the focus of much of the work described here, has C_{3v} symmetry if the first bilayer of the Si surface is considered. When this surface is rotated about its azimuth, where ϕ is defined as the angle between the $[2\bar{1}\bar{1}]$ direction on the (111) face and the projection of the incident wave vector parallel to the surface, the angular dependence in the SH response can be written[22,23]

$$I_{p,p}^{(2\omega)}(\phi)=|a^{(\infty)}+c^{(3)}\cos(3\phi)|^{2}, \qquad (3)$$

$$I_{p,s}^{(2\omega)}(\phi)=|b^{(3)}\sin(3\phi)|^{2}, \qquad (4)$$

where the subscripts refer to the polarizations of the fundamental and SH light, respectively. P polarization refers to the polarization vector of the light residing in the plane of incidence, whereas the polarization vector for s polarization is normal to the plane of incidence. The complex coefficients $a^{(\infty)}$, $b^{(3)}$, and $c^{(3)}$ contain the surface dipole susceptibility elements χ_{ijk}, any contribution from higher order bulk susceptibility terms, γ and ζ, and the appropriate Fresnel factors. The complex coefficient $a^{(\infty)}$ is referred to as the isotropic coefficient as it remains invariant with rotation and contains surface terms χ_{zxx}, χ_{xzx}, χ_{zzz}, and bulk terms γ and ζ. The anisotropic coefficients, $b^{(3)}$ and $c^{(3)}$, include terms which vary with ϕ and contain both χ_{xxx} and ζ.

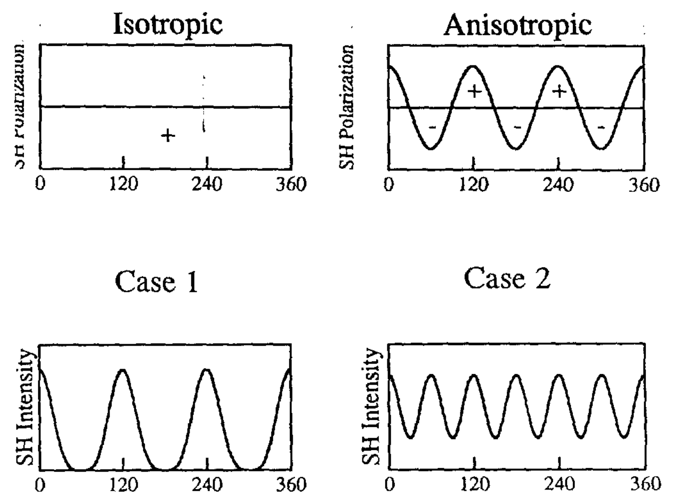

FIG. 1. Demonstration of the interference between isotropic and anisotropic contributions of the same magnitude. (Case 1) If the two polarizations are in phase, their interference will result in three maxima in the rotational pattern. (Case 2) If the polarizations are out of phase by 180°, the resulting anisotropy pattern will have six maxima.

For p-input and p-output polarization the observed intensity modulation upon azimuthal rotation arises from the interference between these anisotropic and isotropic terms. The SH patterns can be understood by considering how these two polarizations interfere, as illustrated in Fig. 1. In this simple example, both the isotropic and anisotropic polarizations are chosen to have the same magnitude. If the polarizations are in-phase (case 1), they will interfere and result in three maxima in the rotational spectrum. If they are out-of-phase by 180°, six maxima are observed (case 2). These are the two extremes since in most cases the contributions are not completely in-phase or out-of-phase. A fit to Eq. (3) yields the ratio $c^{(3)}/a^{(\infty)}$, which contains a magnitude and relative phase angle reflecting this interference under the experimental conditions. Rotational anisotropy measurements under specific polarization conditions are very sensitive to relative changes in both magnitude and phase of either the isotropic or anisotropic contributions.[24,25]

The application of a dc field to the interface as in the case of these studies adds additional factors to the polarizability, where[26]

$$\mathbf{P}_{\text{eff}}^{(2)}(2\omega)=\chi_{\text{eff}}^{(2)}:E(\omega)E(\omega)+\chi_{\text{eff}}^{(3)}:E(\omega)E(\omega)E(\text{dc}). \qquad (5)$$

The potential dependence is expressed in the third order term, where $\mathbf{E}_{\text{dc}}$ is the static electric field oriented normal to the surface. This field is on the order of 1–5 V and drops across the space charge region (SCR) of the semiconductor. The strength of the dc field can be on the order of 10^{6}–10^{7} V/m depending on the depth of the SCR which is governed largely by the doping density of the semiconductor. This can be viewed as a mixing of a static field that induces a polarization strictly oriented in the z direction (normal to the electrode surface) and both the surface and bulk polarization induced by light waves. This additional polarization can be written as the following:[27]

$$\mathbf{P}_i^{(2\omega)}(\mathbf{E}_{l\ \mathrm{dc}})=\chi'^{(3)}_{ijkl}\mathbf{E}_j(\omega)\mathbf{E}_k(\omega)\mathbf{E}_{l\ \mathrm{dc}}. \tag{6}$$

Since both $\chi^{(2)}$ and $\chi'^{(3)}$ have the same symmetry constraints imposed by the electrode surface, the overall symmetry of the response remains unchanged and the net effect is that most tensor elements (including the bulk terms because of the extension of the static field into the bulk semiconductor) will be affected[28,29] by the interfacial charging.

For the general discussion of the observed potential dependence, Eq. (5) can be written in a simpler form as

$$I_{\mathrm{SH}}\propto\|\overleftrightarrow{F}(\chi_B^{(2)}+\chi_S^{(2)}+\chi_{\mathrm{eff}}^{(3)}\Delta\Phi)\|^2, \tag{7}$$

where $\overleftrightarrow{F}$ corresponds to the linear Fresnel factors, $\chi_S^{(2)}$ and $\chi_B^{(2)}$ are the surface and bulk susceptibilities, $\chi_{\mathrm{eff}}^{(3)}\Delta\Phi$ is the effective cubic nonlinearity arising from the static field which includes all terms that vary linearly with field strength.[30] $\Delta\Phi$ is the potential drop across the semiconductor space charge region and is proportional to the difference between the applied (E_{app}) and the flatband (E_{fb}) potential. When the SH response is dominated by the cubic nonlinearity term, the observed potential dependence should be parabolic with a minimum near the flatband potential. Such behavior has been observed in numerous studies of metal/electrolyte systems.[31] Under conditions, where the surface and/or bulk quadratic nonlinearities dominate, parabolic potential dependence with a minimum shifted from flatband would be observed.

III. EXPERIMENTAL CONSIDERATIONS

The optical measurements employ the fundamental output from a 10 Hz Nd:YAG laser which illuminates the surface at a 32° incident angle. 10 ns pulses of $\approx$0.3 J/cm^2 were used, which is below the damage threshold for silicon. The electrochemical cell has described previously,[24] and consists of a three electrode system with the n-Si(111) sample as the working electrode, a platinum wire counter electrode, and the saturated calomel reference electrode (SCE) which is isolated from the working electrode by a ceramic junction. Flatband potentials are determined by photocurrent transients. All potential scans are restricted to the region where stable photocurrent is observed.

For the UHV studies, the sample was mounted on a manipulator capable of 360° azimuthal rotation in a vacuum chamber with a base pressure of 3.5×10^{-9} Torr. The chamber is equipped with an Auger electron spectrometer (AES) and low energy electron diffraction (LEED) to monitor surface cleanliness and crystallinity. For a portion of the studies, the Si surface was cleaned by successive cycles of sputtering (Ne^+, 1 kV, 15 μA) and annealing (1000 K).

The Si(111) wafers used in the experiments are n-doped (phosphorus) with a resistivity of 3.0–6.5 Ω cm, which represents a doping density of $\approx 10^{15}$ cm^{-3}. The 0.66–0.71 mm thick samples are degreased by ultrasonification in separate baths of methylene chloride, acetone, and methanol and then dried with nitrogen. The back of the wafer is etched for 1 min in 48% HF to remove the native oxide and then mounted on Ga–In eutectic that has been placed on an embedded copper contact in a Kel-F shaft. A mask containing an embedded acid resistant fluorocarbon o-ring is used to seal the back surface from the electrolyte. The polished side of the wafer is etched as described below and loaded into the electrochemical cell.

The surface of the silicon wafer is prepared by etching in buffered NH_4F/HF solution (pH=8) which is known to leave the surface atomically smooth and in a mono-H-terminated state.[1,32,33] In contrast, if the surface is etched with HF, the resulting surface is mono-, di-, and tri-H-terminated and consequently is microscopically rough.[7] IR studies have shown that surface roughness gradually diminishes as the pH of the buffered solution is increased, leading to an atomically smooth, ideal mono-H-terminated Si(111) surface at a pH of 8–9.[1] Furthermore, the mono-H-terminated Si(111) surfaces are found to be resistant to oxidation in electrolyte solution (until the surface is subjected to anodic potentials positive of flatband).[5,9,34] After the sample has been etched, it is immersed in 0.1 M NH_4F if the H-terminated surface is to be maintained, or in 0.1 M H_2SO_4 if an oxide is to be grown. Oxides are grown on the Si samples photoanodically by the stepwise increase in potential from the flatband to a final potential of +5.0 V, while keeping the current below 30 μA/cm^2, and illuminating the sample with a diffuse HeNe beam. Thicknesses of the oxides are determined by a combination of ellipsometry, photocurrent measurements, and etchback times. Flatband potentials have been determined by photocurrent transient measurements.

IV. RESULTS

Figure 2 shows the rotational anisotropy in the SH response with p-input and p-output polarization for a Si(111) surface studied in NH_4F at four representative potentials. All samples were etched for 3 min in 2.0 M NH_4F at pH 8.0 to produce a H-terminated surface. *In situ* electrochemical etching of anodically grown oxides shows the surface remains H-terminated in the dark at potentials well positive of flatband in 0.2 M NH_4F.[35] The surface should be relatively free of any photogenerated surface oxides since in fluoride containing electrolytes, the dissolution of this oxide competes with the photo-oxidation process. At all potentials examined the threefold symmetry expected of the (111) surface of a cubic lattice is observed. Figure 2(a) was taken at −0.65 V and a fit to Eq. (3) yields a value for $c^{(3)}/a^{(\infty)}$ of $2.2e^{i21°}$. From current transient measurements, this is determined to be the flatband potential. As the potential is driven positive into the depletion region, the rotational anisotropies show a strong and progressive variation. The magnitude of the ratio of $c^{(3)}/a^{(\infty)}$ changes by approximately a factor of 2 over this 1.35 V region. More striking is the change in the phase angle of the ratio from 22° to 126° over this potential range. The uncertainty in the phase angle measurement is ±5°. At potentials more negative of the flatband, the magnitude of the signal intensity continues to increase although the ratio of $c^{(3)}/a^{(\infty)}$ decreases only slightly. For the H–Si(111) surface, decreasing the potential much beyond flatband (−0.65 V versus SCE) results in significant hydrogen evolution which interferes with the optical process and prevents examination of the sample under accumulation conditions.

To obtain a better understanding of the potential dependence of $c^{(3)}$ and $a^{(\infty)}$ independently, the experiments were

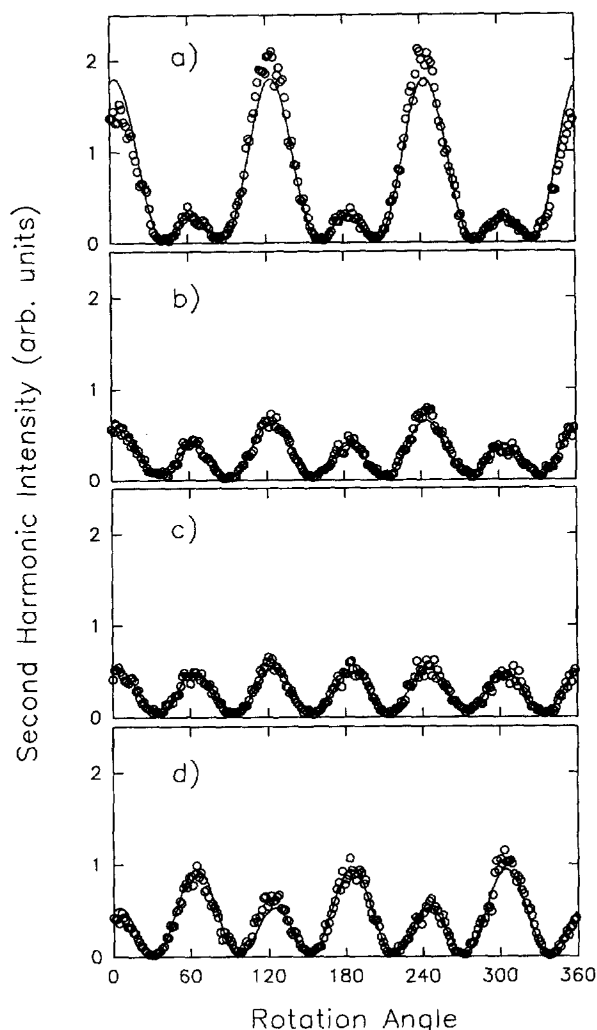

FIG. 2. SH rotational anisotropy from n-Si(111) immersed in 0.1 M NH_4F at flatband and depletion conditions. All scans were taken with p-input and p-output polarizations. The solid line is the fit to Eq. (3), (a) sample biased at the flatband potential, −0.65 V (SCE), $c^{(3)}/a^{(\infty)}=2.2e^{i21°}$; (b) 0.0 V, $c^{(3)}/a^{(\infty)}=3.2e^{i63°}$; (c) +0.2 V, $c^{(3)}/a^{(\infty)}=3.4e^{i86°}$; (d) +1.0 V, $c^{(3)}/a^{(\infty)}=3.8e^{i126°}$.

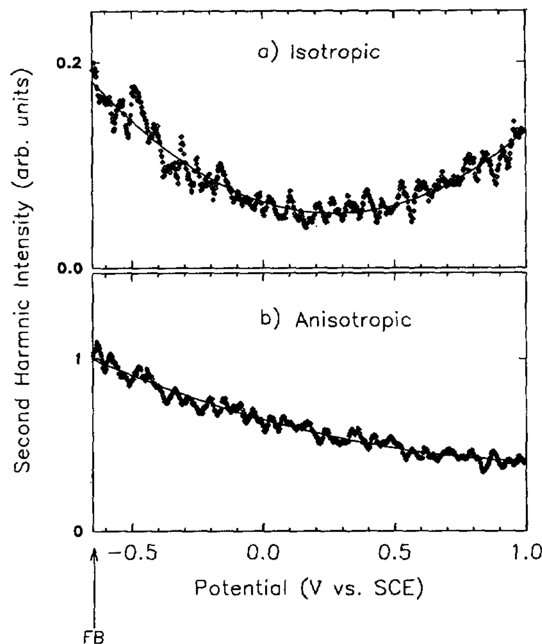

FIG. 3. Potential dependence in the isotropic $a^{(\infty)}$ and anisotropic response $\varepsilon^{(3)}$ for Si(111) prepared in a H-terminated state and biased in 0.1 M NH_4F. The isotropic response was monitored with p-polarized incident light and p-polarized SHG with $\phi=30°$. The anisotropic response was monitored with p-polarized incident light and s-polarized output light at $\phi=30°$.

conducted at $\phi=30°$ which allows isolation of the isotropic and anisotropic contributions. As shown in Fig. 3, both the isotropic and anisotropic response are found to have a parabolic potential dependence with a higher overall signal level from the latter. The isotropic response which would most readily couple to the applied static field has a minimum near +0.26 V, nearly 900 mV from the flatband potential. The field can couple to the depth of the space charge region, which for this surface biased at +0.3 V is on the order of 1200 nm. The anisotropic response has a minimum near +1.6 V, even further away from flatband.

Rotational anisotropy experiments were also conducted in UHV for comparison. A sample was prepared in a H-terminated state prior to mounting in the chamber which was then evacuated to the base pressure. No additional surface cleaning was performed. Figure 4(a) shows the results with a fit to the data giving a phase angle of 61°. The results are similar to that obtained in solution. The best correspondence is for the hydrogen terminated sample in solution which is biased a few hundred millivolts positive of the flatband. After sputtering the sample with Ne^+ and annealing at 900 K, an oxide-free surface with a (7×7) reconstruction was obtained. The SH response from this sample is shown in Fig. 4(b). The reconstructed surface generates a much higher signal at 1064 nm than the nonreconstructed surface with this enhancement attributed to the increase of long range ordering of the surface layer.[4]

Figure 5 shows the results for the Si(111) surface examined at flatband in H_2SO_4. The surface was initially prepared in a H-terminated state. For this system the flatband potential was measured to be −0.6 V. As mentioned previously, the oxides are insoluble in the acid and can form on the surface particularly in the presence of the probe laser light. The response from the surface studied in H_2SO_4 at the flatband potential gives a fit to $c^{(3)}/a^{(\infty)}$ of $1.7e^{i44°}$ and is similar to that obtained in NH_4F [Fig. 2(a)]. From one experiment to the next, a variation in the phase (ranging from 30° to 60°) is observed. The flatband potential is also found to vary slightly in time, shifting anodically with the formation of oxide. Both variations are attributed to photogenerated surface species which can store charge at the interface in an unpredictable manner. This changes the degree of band bending for a given applied potential, thus leading to different results from one experiment to the next. The photocurrent measurements give an estimate of the amount of photogenerated species to be less than 3 ML.

In a similar manner the SH response has been studied from Si(111) surfaces on which varying thicknesses of SiO_2 have been photoanodically grown. Figure 6 displays the ro-

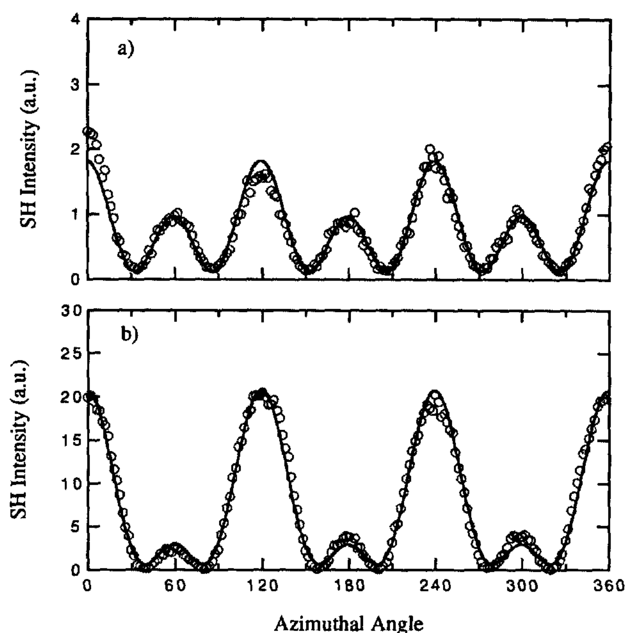

FIG. 4. SH rotational anisotropy from Si(111) initially prepared in a H-terminated state and then transferred to UHV. (a) This sample was loaded into UHV and evacuated to base pressure. No additional cleaning was performed. The result is SH rotational anisotropy from a H-terminated surface in UHV with a fit to $c^{(3)}/a^{(\infty)}=2.8e^{i61°}$. (b) This surface was sputtered (Ne^+) and annealed (900 K) to remove any oxide. The result is theSi(111)-7×7 reconstructed surface with a fit to $c^{(3)}/a^{(\infty)}=1.8e^{i28°}$.

tational anisotropy from an oxide covered surface in H_2SO_4 at four different potentials, 0.0 V [Fig. 6(a)] corresponding to the flatband potential, and three more positive potentials, +1.5, +2.5, and +3.5 V in Figs. 6(b) to 6(d), respectively. For all oxidized samples, the flatband potential shifts anodi-

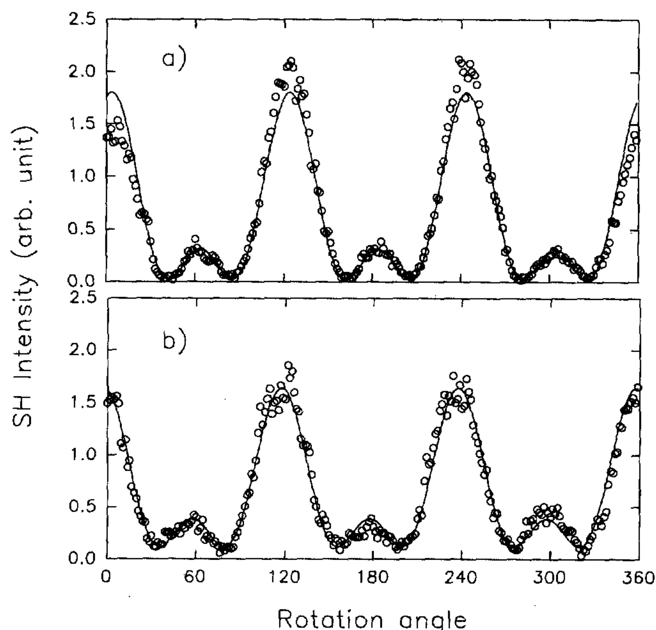

FIG. 5. Rotational anisotropy from n-Si(111) for p-input and p-output polarizations. (a) Si(111) in 0.1 M NH_4F biased at the flatband potential of −0.65 V (SCE). Fitting to Eq. (3) yields $c^{(3)}/a^{\infty}=2.2e^{i21°}$, (b) Si(111) in 0.1 M H_2SO_4 biased at the flatband potential of −0.60 V; $c^{(3)}/a^{(\infty)}=1.7e^{i44°}$.

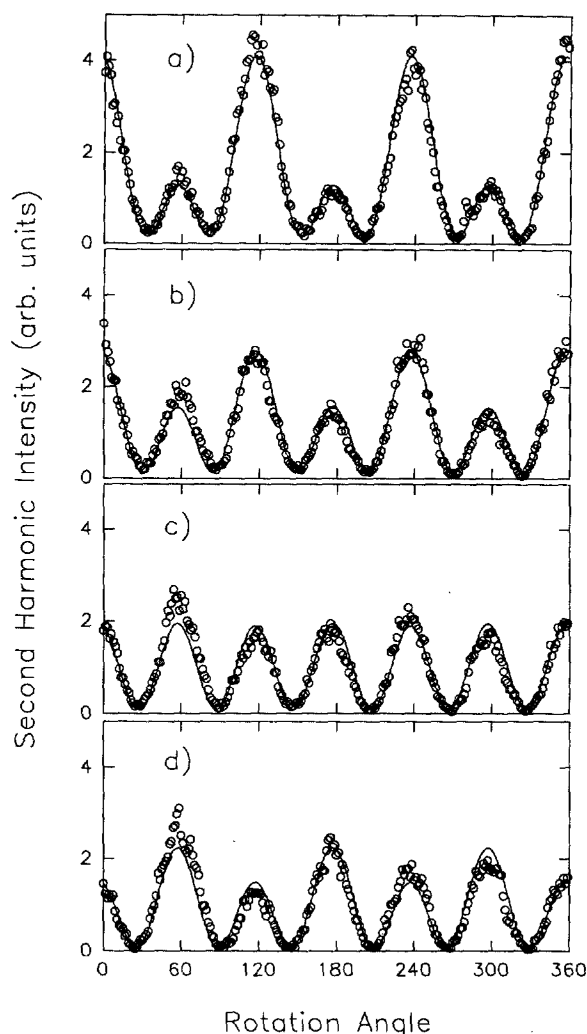

FIG. 6. Potential dependent rotational anisotropy in the p-input and p-output SH response from a 40 Å photoanodically grown oxide (SiO_2) in 0.1 M H_2SO_4. (a) at flatband (0.0 V vs SCE); fit to Eq. (3) yields $c^{(3)}/a^{(\infty)}=2.5e^{i41°}$, (b) +1.5 V from flatband, $c^{(3)}/a^{(\infty)}=3.4e^{i58°}$, c) +2.5 V from flatband, $c^{(3)}/a^{(\infty)}=4.5e^{i92°}$, (d) +3.5 V from flatband, $c^{(3)}/a^{(\infty)}=4.8e^{i120°}$.

cally as determined by the current transient measurements. The potential "window" for studying the oxide-coated surfaces widens due to the insulating nature of the overlayer. The oxide layer is estimated to be ~40 Å based on ellipsometry measurements and etchback times. Because the electrochemically grown oxides have substantial water content in the first monolayers of oxide, with this ratio decreasing as the thickness increases,[17] the ellipsometrically determined thicknesses are viewed as an upper limit.

In comparing the response from the Si(111) surfaces of Fig. 2(a) measured at flatband with the oxidized sample in Fig. 6(a), two important observations can be made. The rotational anisotropy persists in the presence of the oxide and the signal from the oxide covered surface is enhanced relative to the more oxide free sample in Fig. 1(b). The former observation suggests that in the presence of the oxide, the signal from Si(111) continues to dominate the response over the more isotropic and disordered oxide overlayer. The signal

enhancement observed in the presence of oxide indicates that the SHG is sensitive to the Si(111) surface adjacent to the oxide and that it is not merely a bulk response. However, the possibility does exist that the signal enhancement is due to a change in the Fresnel factors which occurs as the oxide grows on the surface, thus altering the angle of incidence of the incoming optical field and therefore increasing the SH response.

As with the Si(111) surfaces, there is a strong potential dependence in the response from the Si(111)/SiO_2 interface as manifested in both the relative magnitude and phase of the rotational anisotropy. For an applied bias of +3.5 V beyond the flatband potential (0.0 V for this sample), the relative phase angle between the anisotropic and isotropic response changes by 80°. For the H-terminated surface, the change in phase angle occurs over a much smaller potential range of 1.35 V. For 15 and 25 Å samples, a similar phase shift of 80° occurs over a potential range of 2.0 and 2.5 V, respectively. At flatband, the fits of the anisotropies for the different oxide covered samples are nearly the same. The observed trend is that the thicker the oxide overlayer, the smaller is the observed change in phase per unit voltage dropped across the interface.

The potential dependence of the anisotropic and isotropic response was independently examined for these oxidized samples. Both exhibit a potential dependence similar to Fig. 3, with minima which are well removed from the flatband potential. For the 40 Å thick oxide sample, the measured minima in the anisotropic and isotropic response occurs near +3.3 and +2.2 V, respectively; both minima occur far from the flatband potential at 0.0 V.

V. DISCUSSION

The results of the electrochemical studies described above demonstrate the sensitivity of SHG to the Si(111) surface whether it is adjacent to an electrolyte solution or various thicknesses of oxides. Fits to the rotational anisotropy data obtained as a function of potential show that SHG is sensitive to the applied field within the depletion layer and that both the amplitude and the relative phase of the response vary with potential. For all electrochemical studies, both the anisotropic and isotropic response display a parabolic potential dependence. The fact that the minimum of the isotropic or anisotropic signal does not occur at the flatband for either the H_2SO_4 or NH_4F solutions suggests that terms other than $\chi_{\text{eff}}^{(3)}\Delta\Phi$ in Eq. (7) must be contributing. $\chi_B^{(2)}$ is the most likely factor considering that the penetration depth of the pump light is on the order of 1 cm, considerably deeper than the SCR. Previous studies in air have determined that the SH contribution from the surface and the bulk of Si(111) are of similar magnitude.[23,36] Further evidence for the importance of the bulk response comes from the observation that when Si(111) surfaces are roughened by etching in 48% HF prior to introduction into the NH_4F, the rotational anisotropies for the roughened and unroughened samples are quite similar. There is no evidence of an isotropic response from a disordered silicon surface superimposed on the response from the crystalline lattice. The intensity of the overall response is however slightly larger in the roughened case, suggesting that $\chi_s^{(2)}$ is not insignificant. Analysis of the response in Fig. 3 based on Eq. (7) indicates that the sum of $(\chi_s^{(2)}+\chi_B^{(2)})$ is at least of comparable magnitude to the contribution from $\chi_{\text{eff}}^{(3)}\Delta\Phi$.

In an earlier work,[26] it appears that the potential drop in the SCR was assumed to be relative to the absolute applied potential, not the flatband potential, and a model of quadratic dependence of the SHG with applied potential was found to fit the data. Although the flatband was not measured in the earlier studies, the current–voltage data presented suggests that the flatband potential was well negative of 0 V (versus SCE). With this correction, the data clearly do not fit a quadratic dependence in applied field strength, but does resemble the data reported here. Furthermore, the earlier studies[26,37] were performed without specified polarization and sample orientation information which make comparisons difficult.

An issue that must be addressed is the effect of the probe light on the surface reactivity, particularly in H_2SO_4 where the photogenerated oxides are insoluble. The influence of the intense 1.064 μm pump radiation must be considered since it is above the band gap for Si. With most samples, the signal-to-noise ratio of the data improves markedly after the completion of one to three rotational scans (4–12 min). Photocurrent transients are observed at all potentials, although near flatband they are small and bipolar. These transients reach a steady state at any fixed potential. Near flatband the integrated charge in each photocurrent transient is approximately 10^{-7} C (10^{-6} C/cm^2/laser shot). Assuming a quantum yield of one for the oxidation of Si, a four electron process, this indicates that 3000 laser shots will oxidize a monolayer of Si, and thus a period of 12 scans would be required to oxidize a monolayer. This means that the oxide thickness in H_2SO_4 is less than 3 ML. In NH_4F, our observations suggest the surface is essentially oxide-free. Earlier work[38] has shown a slightly porous hydrogen terminated surface grows on the silicon surface under continuous illumination when biased positive of flatband, but etches away when immersed in NH_4F in the dark. The low duty cycle of the illumination used in these experiments would produce a steady state close to the nonporous surface condition. Consequently, no change is observed in the phase at a fixed potential before and after allowing a sample to sit in the dark for a period of 20 min.

The effect of the oxide is clearly evident in the potential dependence of the SHG. Compared to the relatively oxide-free sample, a larger bias must be imposed across the interface to obtain a relative phase comparable to that of the H-terminated surface. At flatband, the fits to the anisotropies for the different oxide covered samples show little variation as one would expect since $(\chi_s^{(2)}+\chi_B^{(2)})$ should be the similar for samples with more than a few monolayers of SiO_2. The fact that the surface in NH_4F has a slightly different magnitude and phase [Fig. 1(a)] than the H_2SO_4 case is consistent with a different $\chi_s^{(2)}$ due to the presence of oxidized surface species. At potentials positive of flatband, a progressively larger V_{app} is necessary to achieve the magnitude and phase angle that is obtained for surfaces with thinner oxide coatings. For example, an additional +1.0 V must be applied to the 40 Å sample to obtain a phase angle comparable to that

obtained for the 25 Å sample biased at the lower voltage. We attribute the potential dependence in the relative phase to the variation of the field at the surface and within the SCR of the semiconductor. Because of the insulating nature of the oxide, the field at the $Si(111)/SiO_2$ interface is no longer $\Delta\Phi$ but is reduced by the potential drop across the oxide layer V_{ox}. This suggests, for example, that the additional 15 Å of oxide on the surface screens ~1 V of the overall applied field relative to the 25 Å sample.

For the UHV studies the response from the H-terminated surface is similar to that in solution under conditions, where a 100–200 mV bias is applied. The SH experiments thus indicate that in UHV the surface is not at flatband. Two plausible mechanisms for this include the existence of surface states or the charging of the surface (or contaminant species thereon) from stray electrons in the chamber.

We conclude that the potential dependence predominantly originates in the bulk SCR of the semiconductor. It is conceivable that changes in the Fresnel coefficients of the oxide, especially as the oxide thickness increases, could also account for this potential dependence. However, since the complex part of the dielectric for SiO_2 varies to a negligible extent for the wavelength region employed here, there is very little to no absorption by the oxide. Therefore, the changes in the Fresnel factors would be expected to have only a minor effect. Clearly the bulk band bending induced by the static electric field is the major contributor to the potential dependence observed here.

VI. CONCLUSIONS

The studies presented here demonstrate the potential dependence of n-Si(111) samples in different electrochemical environments. The most striking result is the clear dependence of the phase of the SH response on the field present in the SCR. The ability to optically probe, via SH phase measurements, the static electric field in the presence of oxide on the surface has not been demonstrated previously. In contrast to amplitude measurements, phase measurements are a more accurate means of comparing surface changes from one environment to another since the phase will not be affected by nonsignal generating elements in the optical path.

The amplitudes of the isotropic and anisotropic response were shown to be parabolic in agreement with earlier work. However, the more detailed studies reported here demonstrate that there is a significant shift in the minimum in the response relative to the flatband potential. This result demonstrates that there is a much larger contribution from second order terms than assumed previously. The parabolic nature of the response persists with an oxide overlayer but, extends over a considerably wider potential range due to the insulating nature of the oxide. This is consistent with the screening of the applied potential by the oxide which would lead to reduced band bending in the SCR for any given potential. The oxide itself does not appear to optically interfere.

The most significant result is that the phase of the SHG signal for the buried interface is directly correlated with the field in the SCR. Away from resonance this provides a unique probe of the electronic environment at the surface applicable under a variety of conditions including UHV, air, and in solution, for both clean, H-terminated, and oxidized samples. No other single measurement technique is applicable in all these environments for the determination of such a fundamental property of the surface.

ACKNOWLEDGMENT

The authors gratefully acknowledge funding from the Department of Energy, Basic Energy Sciences (DE-FG06-86ER45273).

Presented at the 40th National Symposium of the American Vacuum Society, Orlando, FL, 15–19 November 1993.

[1] P. Jakob, Y. J. Chabal, K. Raghavachari, R. S. Becker, and A. J. Becker, Surf. Sci. **275**, 407 (1992).
[2] G. S. Higashi, Y. J. Chabal, G. W. Trucks, and K. Raghavachari, Appl. Phys. Lett. **56**, 656 (1990).
[3] T. F. Heinz, M. M. T. Loy, and W. A. Thompson, Phys. Rev. Lett. **54**, 63 (1985).
[4] T. F. Heinz, M. M. T. Loy, and W. A. Thompson, J. Vac. Sci. Technol. B **3**, 1467 (1985).
[5] K. Itaya, R. Sugawara, Y. Morita, and H. Tokumoto, Appl. Phys. Lett. **60**, 2534 (1992).
[6] P. Allongue, H. Brune, and H. Gerischer, Surf. Sci. **275**, 414 (1992).
[7] G. S. Higashi, R. S. Becker, Y. J. Chabal, and A. J. Becker, Appl. Phys. Lett. **58**, 1656 (1991).
[8] S.-L. Yau, F.-R. F. Fan, and A. J. Bard, J. Electrochem. Soc. **139**, 2825 (1992).
[9] E. Tomita, N. Matsuda, and K. Itaya, J. Vac. Sci. Technol. A **8**, 534 (1990).
[10] U. Memmert and R. J. Behm, Festkoerperprobleme **31**, 189 (1991).
[11] Y. Kim and C. M. Lieber, J. Am. Chem. Soc. **113**, 2333 (1991).
[12] P. R. Fischer, J. L. Daschbach, and G. L. Richmond, Chem. Phys. Lett. **218**, 200 (1994).
[13] N. Sorg, J. Kruger, W. Kautek, and J. Reif, Ber. Bunsenges. Phys. Chem. **97**, 402 (1993).
[14] W. Daum, H.-J. Krause, U. Reichel, and H. Ibach, Phys. Rev. Lett. **71**, 1234 (1993).
[15] G. L. Richmond, J. M. Robinson, and V. L. Shannon, Prog. Surf. Sci. **28**, 1 (1988).
[16] G. L. Richmond, in *Optical Second Harmonic Generation as an In Situ Probe of Electrochemical Interfaces*, edited by A. J. Bard (Marcel Dekker, New York, 1991).
[17] H. J. Lewerenz, Electrochim. Acta **37**, 847 (1992).
[18] P. S. Pershan, Phys. Rev. **130**, 919 (1963).
[19] P. Guyot-Sionnest and Y. R. Shen, Phys. Rev. B **38**, 7985 (1988).
[20] Y. R. Shen, *The Principles of Nonlinear Optics* (Wiley, New York, 1984).
[21] Y. R. Shen, Nature **337**, 519 (1989).
[22] J. E. Sipe, D. J. Moss, and H. M. Van Driel, Phys. Rev. B **35**, 1129 (1987).
[23] H. W. K. Tom, Ph.D. dissertation, University of California, Berkeley, 1984.
[24] G. L. Richmond, in *Second Harmonic Generation as an In-situ Probe of Single Crystal Electrode Surfaces*, edited by H. Gerischer and C. W. Tobias (VCH, 1992).
[25] R. Georgiadis, G. A. Neff, and G. L. Richmond, J. Chem. Phys. **92**, 4623 (1990).
[26] C. Lee, R. K. Chang, and N. Bloembergen, Phys. Rev. Lett. **18**, 167 (1967).
[27] D. A. Koos, V. L. Shannon, and G. L. Richmond, J. Phys. Chem. **94**, 2091 (1990).
[28] R. A. Bradley, R. Georgiadis, S. D. Kevan, and G. L. Richmond, J. Chem. Phys. **99**, 5535 (1993).
[29] J. Qi, M. S. Yeganeh, I. Koltover, A. G. Yodh, and W. M. Theis, Phys. Rev. Lett. **71**, 633 (1993).
[30] P. Guyot-Sionnest and A. Tadjeddine, J. Chem. Phys. **92**, 734 (1990).

[31]G. L. Richmond, in Ref. 16.
[32]G. S. Higashi, Y. J. Chabal, G. W. Trucks, and K. Raghavachari, Appl. Phys. Lett. **56**, 656 (1990).
[33]P. Jakob and Y. J. Chabal, J. Chem. Phys. **95**, 2897 (1991).
[34]R. Houbertz, U. Memmert, and R. J. Behm, Appl. Phys. Lett. **58**, 1027 (1991).
[35]H. J. Lewerenz and T. Bitzer, J. Electrochem. Soc. **139**, L21 (1992).
[36]H. W. K. Tom, T. F. Heinz, and Y. R. Shen, Phys. Rev. Lett. **51**, 1983 (1983).
[37]O. A. Aktsipetrov and E. D. Mishina, Sov. Phys. Dokl. **29**, 37 (1984).
[38]L. M. Peter, D. J. Blackwood, and S. Pons, Phys. Rev. Lett. **62**, 308 (1989).